Journal of Zhejiang University-SCIENCE A (Applied Physics & Engineering)
ISSN 1673-565X (Print); ISSN 1862-1775 (Online)
www.zju.edu.cn/jzus; www.springerlink.com
E-mail: jzus@zju.edu.cn

Destruction of hexafluoroethane in a dielectric-packed bed plasma reactor

D. H. KIM[1], Y. S. MOK[†‡1], S. B. LEE[1], S. M. SHIN[2]

([1]*Department of Chemical & Biological Engineering, Research Institute of Advanced Technology, Jeju National University, Jeju 690-756, Korea*)

([2]*Environmental Business Unit, Samsung Engineering Co., Ltd., Hwasung, Gyeonggido, Korea*)

[†]E-mail: smokie@jejunu.ac.kr

Received Nov. 30, 2009; Revision accepted Jan. 21, 2010; Crosschecked June 3, 2010

Abstract: The destruction of hexafluoroethane (C_2F_6), also known as R-116, was investigated in a nonthermal plasma reactor packed with dielectric pellets. The effects of the feed gas composition and the input power on the destruction of C_2F_6 were examined. The feed gas composition was varied by changing the oxygen content, the argon content and the initial C_2F_6 concentration. An increased input power led to increased C_2F_6 destruction as a result of promoting the electron-molecule collisions to dissociate C_2F_6 molecules. The addition of argon to the feed gas greatly improved the C_2F_6 destruction by reducing the energy losses due to vibrational excitation and dissociation of N_2 molecules, while the increases in the oxygen content and the initial C_2F_6 concentration decreased the destruction efficiency. The byproducts including CO_2, CO, COF_2, CF_4, SiF_4, NO_2, and N_2O were identified, and the destruction mechanisms were elucidated, referring to these compounds. The most abundant byproduct was found to be carbonyl fluoride (COF_2), indicating that it serves as an important medium to convert C_2F_6 into CO_2. The energy requirement for the C_2F_6 destruction was in the range of 8.2–45.3 MJ/g, depending on the initial concentration.

Key words: Hexafluoroethane (C_2F_6), Nonthermal plasma, Gas composition, Destruction mechanisms
doi:10.1631/jzus.A0900734 **Document code:** A **CLC number:** O613.41; O539

1 Introduction

Perfluorocarbons (PFCs) such as CF_4, C_2F_6, and C_3F_8 that have been used as dry-etch gases in the semiconductor industry contribute significantly to global warming. Hexafluoroethane (C_2F_6) is a particularly versatile etchant for many substrates in semiconductor manufacturing. It has a global warming potential that is 11900 times greater than carbon dioxide. Regarding the abatement of C_2F_6, several technologies including thermal destruction, catalytic destruction, adsorption, thermal plasma and nonthermal plasma have been applied (Hartz *et al*., 1998; Delattre *et al*., 1999; Tsai *et al*., 2002; Lee and Choi, 2004; Takaki *et al*., 2006). C_2F_6 is chemically inert and thermally stable, which is attributed to the strength of the C-F bond and the shielding effect of the fluorine atoms. Thus, thermally destroying its molecular structure requires very high temperatures, over 1300 K. The use of a catalyst can lower the operation temperature by decreasing the activation energies of relevant reactions, but the catalyst poisoning due to the destruction products may be a significant problem in practice. Thermal plasma processes may be useful techniques, especially for high concentration streams (Sun and Park, 2003; Mizeraczyk *et al*., 2005), but there are several disadvantages of using thermal plasma, such as electrode erosion and high energy consumption. Nonthermal plasma reactors have also been used for destroying fluorocarbons (Chang and Yu, 2001; Takaki *et al*., 2006; Chen *et al*., 2008; Mok *et al*., 2008). The main problem of nonthermal plasma lies in low PFC destruction efficiency, but combinations of nonthermal plasma with other technologies could

‡ Corresponding author
© Zhejiang University and Springer-Verlag Berlin Heidelberg 2010

significantly improve destruction efficiency. Chang *et al*. (2001) introduced catalysis for the purpose of enhancing the effectiveness of nonthermal plasma, and Urashima *et al*. (2001) proposed a two-stage process consisting of nonthermal plasma and adsorption.

Although there have been several reported works on the destruction of C_2F_6, few have dealt with the gas composition effect and the destruction mechanisms. In this work, a nonthermal plasma reactor packed with dielectric pellets was applied to the destruction of C_2F_6. Using this experimental set-up, the objectives of this study were to investigate the effect of the gas composition and input power on the destruction of C_2F_6, and to elucidate the destruction mechanisms.

2 Experimental

The dielectric-packed bed plasma reactor for destroying C_2F_6 is schematically shown in Fig. 1. The plasma reactor consisted of a quartz tube with inner and outer diameters of 21 mm and 24 mm, respectively, an 8-mm stainless steel screw, and 3-mm alumina balls (Daihan Scientific, Korea) as dielectric packing material. The alumina balls (93% Al_2O_3) are the same as those used for grinding media in ball milling. The outer surface of the quartz tube was wrapped with aluminum foil. The effective reactor length was 130 mm, corresponding to the height of the aluminum foil. The void fraction in the reactor was about 0.4. An AC high voltage (frequency 1 kHz) was applied to the stainless steel screw acting as the discharging electrode, and the aluminum foil was connected to the ground electrode. The applied voltage was varied from 10 to 16 kV (peak value) to change the power delivered to the plasma reactor. The plasma reactor was equipped with a water jacket, thereby removing the heat generated during the operation. The voltage applied to the discharging electrode was measured with a 1000:1 high voltage probe (P6015, Tektronix, USA) and a digital oscilloscope (TDS 3032, Tektronix, USA). The input power defined as the amount of electrical power that is delivered to the high voltage transformer was measured by a digital power meter (Yokogawa WT200, Japan). The power consumed in the dielectric-packed bed plasma reactor (i.e., discharge power) can be determined using the Lissajous figure. Under the present experimental conditions, the discharge power was about 60% of the input power.

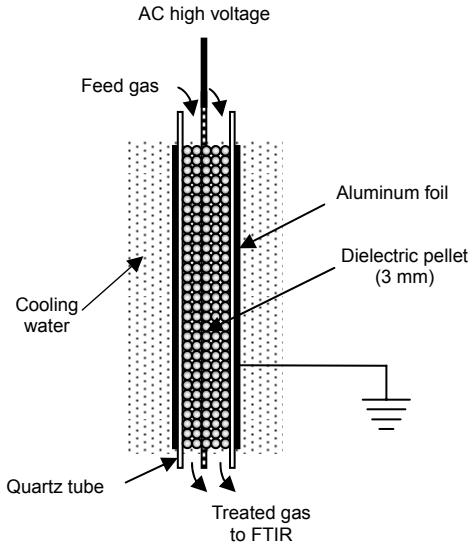

Fig. 1 Schematic diagram of the dielectric-packed bed plasma reactor
FTIR: Fourier transform infrared spectroscopy

The feed gas entering the plasma reactor was formed with C_2F_6, oxygen, argon and nitrogen as the balance gas. The flow rates of those gases were regulated by mass flow controllers (MKS Instruments, Inc., USA). The total flow rate of the feed gas was adjusted to 500 cm^3/min. Considering the void fraction, the residence time of the feed gas in the reactor was calculated to be 1.85 s. The concentration of C_2F_6 was changed from 500×10^{-6} to 2000×10^{-6}, and the oxygen content from 0 to 5.0% (v/v). Argon content was changed up to 20% (v/v). The total flow rate of the feed gas remained constant at 500 cm^3/min, regardless of the changes in the gas composition. The gas treated in the plasma reactor was directed to the Fourier transform infrared spectroscopy (FTIR) spectrometer (Model 1600 Series, Perkin-Elmer, USA) equipped with a long path gas cell (Pike Technologies, Inc., USA) for analyzing the concentrations of C_2F_6 and the byproducts. The intensity of infrared absorbance at a characteristic wavenumber for a certain compound is proportional to its concentration. The C_2F_6 destruction efficiency was determined by comparing the final and initial concentrations.

3 Results and discussion

Fig. 2 shows the dependence of the input power on the applied voltage at different argon contents. The input power was changed from 100 to 250 W by changing the voltage. The voltage/power characteristics somewhat depended on the argon content. Below 200 W, a higher voltage was required to obtain the same input power at lower argon contents, which can be explained by higher plasma inception voltage at lower argon content. On the other hand, above 200 W, the effect of the argon content was reversed, i.e., lower argon contents required lower voltages to obtain the same input power. For instance, at argon contents of 0%, 5%, 10% and 20% (v/v), the voltages required to obtain 250 W were 14.6, 14.8, 15.1, and 15.2 kV, respectively. The datasets given below were obtained by adjusting the input power to desired values.

Fig. 3 presents the destruction efficiency and the amount of C_2F_6 destroyed at different input powers in the range of 100–250 W. The amount of C_2F_6 destroyed is calculated by multiplying the destruction efficiency by the initial C_2F_6 concentration. The general trend was that the destruction efficiency and the amount destroyed increased proportionally with the increase in the input power. The nonthermal plasma produces various radicals, ions and excited molecules. The removal pathways for most of common air pollutants, such as nitrogen oxides, volatile organic compounds (VOCs), and odors are explained by the reactions with these reactive species (Okubo *et al*., 2007; Futamura and Sugasawa, 2008; Yoshida *et al*., 2009). On the other hand, the reactivity of C_2F_6 with these reactive species is extremely low because of its chemical stability. The only process for initiating the destruction of C_2F_6 is believed to be the dissociation by the energetic electrons generated by the plasma, which can be given as (Motlagh and Moore, 1998)

$$e+C_2F_6 \rightarrow CF_3+CF_3+e, \quad (1)$$

$$e+C_2F_6 \rightarrow C_2F_5+F+e. \quad (2)$$

The bond dissociation energies of C-C and C-F are 3.6 and 5.1 eV, respectively, indicating that reaction (1) is superior to reaction (2). According to the mass spectrum of C_2F_6 that illustrates the cracking pattern of this molecule in a mass spectrometer (NIST, 2009),

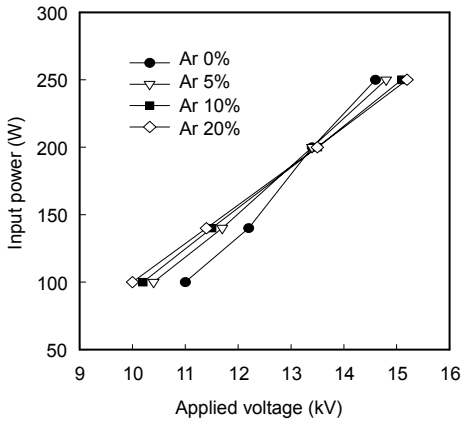

Fig. 2 Dependence of the input power on the applied voltage at different argon contents

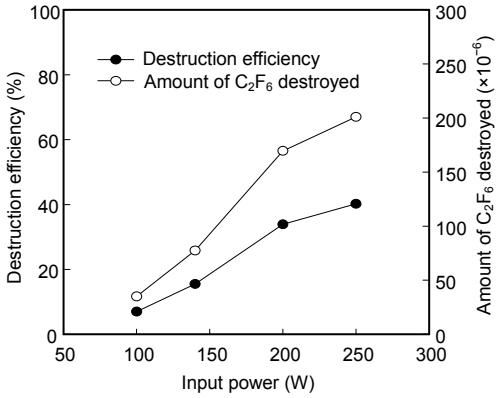

Fig. 3 Effect of the input power on the destruction efficiency and the amount of C_2F_6 destroyed (initial C_2F_6: 500×10^{-6}; oxygen: 0.5% (v/v); argon: 20% (v/v))

the most abundant fragment is that with *m*/*z* 69, corresponding to CF_3, which also supports the observation that reaction (1) is the predominant electron impact dissociation process. The rate of the electron impact dissociation depends on the electron energy and concentration, and thus it stands to the reason that the increased input power should result in greater destruction efficiency (Fig. 3).

The effect of the gas composition on the C_2F_6 destruction is shown in Fig. 4. With the initial C_2F_6 concentration remained constant at 500×10^{-6}, the oxygen content was changed up to 5% (v/v), and the argon content up to 20% (v/v). The C_2F_6 destruction gradually decreased with an increase in the oxygen content. This decrease in the C_2F_6 destruction in the presence of oxygen can partly be explained by the electron attachment to oxygen molecules. As well, the formation of oxygen containing byproducts, such as NO_2 and N_2O, can consume the electrical energy

delivered to the plasma reactor, which may be another reason for lower C_2F_6 destruction at higher O_2 content. For a given oxygen content, the C_2F_6 destruction increased as the argon content increased. This is related to the electron energy distribution. At a low argon content, a large portion of electron energy is lost due to vibrational excitation and dissociation of N_2 molecules (Kucukarpaci and Lucas, 1979), resulting in low destruction efficiency. As the argon content increases, such losses of electron energy decrease, and thus more energetic electrons can participate the C_2F_6 destruction.

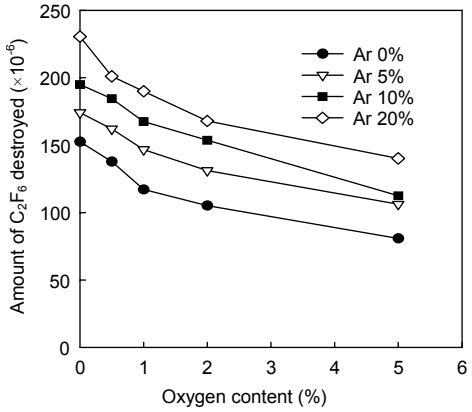

Fig. 4 Effect of the gas composition on the C_2F_6 destruction (initial C_2F_6: 500×10^{-6}; input power: 250 W)

Fig. 5 shows the FTIR spectra of the gas treated in the plasma reactor for different oxygen contents. The C_2F_6 destructions products included CO_2, CO, COF_2, CF_4, and SiF_4. The evolution of SiF_4 is associated with etching of the quartz wall (SiO_2) of the reactor by fluorine (Urashima *et al*., 2001). In addition, nitrogen oxides such as N_2O and NO_2 were identified in the spectra, which increased in concentration with the increasing oxygen content. The reaction pathways leading to the formations of CO_2, CO, COF_2, and CF_4 are explained below. The rate coefficients of the relevant reactions are reported in (Barker, 1995; Mallard *et al*., 1998). The CF_3 radical produced by the electron impact dissociation (reaction (1)) reacts with oxygen to form trifluoromethyl peroxy radical (CF_3O_2):

$$CF_3+O_2\rightarrow CF_3O_2,\ 2.4\times10^{12}\ cm^3/(mol\cdot s). \quad (3)$$

The trifluoromethyl peroxy radical further reacts to form trifluoromethoxy radical (CF_3O) as

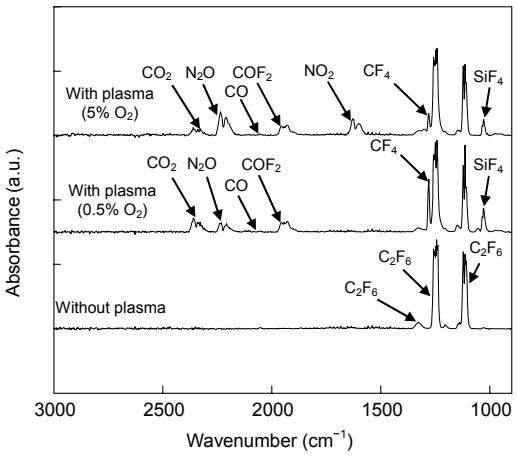

Fig. 5 FTIR spectra of the gas treated in the plasma reactor for different oxygen contents (initial C_2F_6: 500×10^{-6}; argon: 5% (v/v); input power: 250 W)

$$CF_3O_2+CF_3O_2\rightarrow2CF_3O+O_2,\ 1.36\times10^{12}\ (mol\cdot s)^{-1}, \quad (4)$$
$$CF_3O_2+NO\rightarrow CF_3O+NO_2,\ 9.6\times10^{12}\ (mol\cdot s)^{-1}. \quad (5)$$

Note that NO involved in reaction (5) is formed from nitrogen and oxygen by the electrical discharge. The mechanism for the formation of NO has been discussed (Mok *et al*., 2000; Ricketts *et al*., 2004). The trifluoromethoxy radical resulting from reactions (4) and (5) are further degraded to give COF_2:

$$CF_3O+O_2\rightarrow COF_2+FO_2,\ 1.0\times10^{6}\ (mol\cdot s)^{-1}, \quad (6)$$
$$CF_3O+NO\rightarrow COF_2+NOF,\ 3.2\times10^{13}\ cm^3/(mol\cdot s), \quad (7)$$
$$CF_3O+NO_2\rightarrow COF_2+NO_2F,\ 1.9\times10^{12}\ cm^3/(mol\cdot s). \quad (8)$$

Even though the rate constant of reaction (6) is small, its reaction rate can be significant when the oxygen content is high. Other channels for COF_2 formation are as follows:

$$CF_3+O\rightarrow COF_2+F,\ 1.9\times10^{13}\ cm^3/(mol\cdot s), \quad (9)$$
$$CF_3+NO_2\rightarrow COF_2+NOF,\ 1.5\times10^{13}\ cm^3/(mol\cdot s). \quad (10)$$

Further reaction of COF_2 with excited oxygen atom leads to CO_2, and a part of CO_2 can be converted into CO:

$$COF_2+O(^1D)\rightarrow CO_2+F_2,\ 1.3\times10^{13}\ cm^3/(mol\cdot s), \quad (11)$$
$$CO_2+N(^2D)\rightarrow CO+NO,\ 2.2\times10^{11}\ cm^3/(mol\cdot s). \quad (12)$$

The amount of CO was found to be relatively small, compared to other byproducts. The reaction to

form CF_4 is believed to be

$$CF_3+F\rightarrow CF_4,\ 1.2\times10^{13}\ cm^3/(mol\cdot s). \quad (13)$$

In the C_2F_6 destruction, the rate-determining step is reaction (1). Though the succeeding reactions (3)–(13) are relatively fast, the slow rate of reaction (1) controls the overall C_2F_6 destruction rate. In Fig. 6, the destruction mechanisms explained are schematically described.

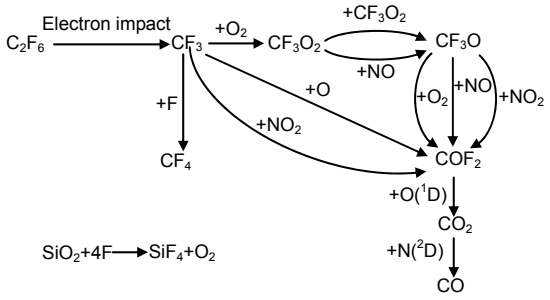

Fig. 6 Plausible reaction pathways responsible for the C_2F_6 destruction

Fig. 7 shows the effect of the initial C_2F_6 concentration on the destruction efficiency and the amount of C_2F_6 destroyed, where the results obtained with and without oxygen are compared. The initial C_2F_6 concentration was varied from 300×10^{-6} to 2000×10^{-6}. In the absence of oxygen, the destruction efficiency decreased with the increase in the initial concentration, more sharply than in the presence of it. The amount of C_2F_6 destroyed in the absence of oxygen showed its maximum at an initial concentration of 1000×10^{-6}, and then decreased as a result of the sharp decrease in the destruction efficiency. It is natural that the destruction efficiency should decrease with increases in the initial C_2F_6 concentration, because of the decrease in the relative amount of energetic electrons available for the destruction. What should be noted in Fig. 7 is the extent of the decrease in the destruction efficiency according to the initial C_2F_6 concentration. In the absence of oxygen, the C_2F_6 destruction efficiency was much more sensitive to the change in its initial concentration. When the initial concentration was changed from 300×10^{-6} to 2000×10^{-6}, the destruction efficiency decreased from 40% to 32.5% with oxygen, whereas it changed from 51% to 21% without oxygen. This result may be explained by reaction (3) and succeeding reactions. The CF_3 radicals formed by reaction (1) can recombine with each other. Since the recombination reaction is necessarily more probable at higher C_2F_6 concentrations, the destruction efficiency decreases as the initial C_2F_6 concentration increases. In the presence of oxygen, however, there is less possibility of the CF_3 radicals recombining, because oxygen scavenges them quickly, as given in reaction (3). That is why the C_2F_6 destruction efficiency obtained in the absence of oxygen was much more sensitive to the change in its initial concentration.

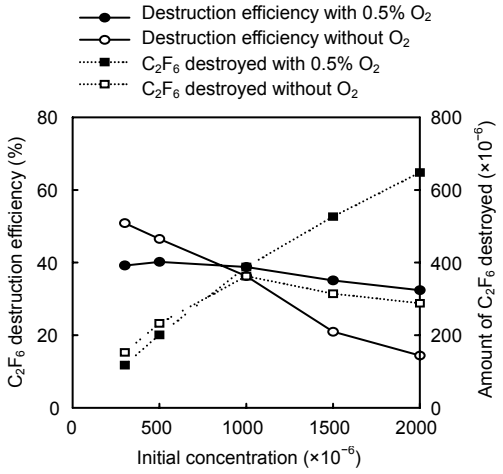

Fig. 7 Effect of the initial C_2F_6 concentration on the destruction efficiency and the amount destroyed (argon: 20% (v/v); input power: 250 W)

Table 1 summarizes the energy requirements to destroy 1 g of C_2F_6 at various initial concentrations, which ranged from 8.2 to 45.3 MJ/g, depending on the initial concentration. The energy requirements reported by Urashima *et al*. (2001) and Takaki *et al*. (2004) are in the range of 2.5–3.7 g/(kW·h), tantamount to 0.97–1.44 MJ/g (initial C_2F_6 concentration: 3000×10^{-6}). These values are much smaller than those summarized in Table 1, but it should be noted that there are many parameters such as initial C_2F_6

Table 1 Energy requirement for the C_2F_6 destruction

Initial C_2F_6 ($\times10^{-6}$)	Amount of C_2F_6 destroyed ($\times10^{-6}$)	Energy requirement (MJ/g)
300	118	45.3
500	201	26.5
1000	388	13.7
1500	526	10.1
2000	648	8.2

Oxygen: 0.5% (v/v); argon: 20% (v/v); input power: 250 W

concentration, AC frequency, gas composition, reaction temperature, and reactor geometry that can affect the energy requirement.

Fig. 8 presents the concentrations of the byproducts obtained by changing the initial C_2F_6 concentrations. The concentrations of all byproducts increased with greater initial C_2F_6 concentrations. As understood from Fig. 8, COF_2 is the major byproduct. COF_2 is formed by reactions (3)–(10), and it can further decompose into CO_2 by reaction (11). Under these experimental conditions, about 10% of the C_2F_6 destroyed was converted into CF_4 (reaction (13)). If all of the C_2F_6 destroyed was converted into CO_2, COF_2 and CF_4, the sum of these compounds should amount to twice as much as the amount of C_2F_6 destroyed, on the basis of carbon balance. But the byproducts in Fig. 8 accounted for only about 70% of the C_2F_6 destroyed. Though not fully discussed here, chemical pathways leading to other byproducts like particulate matters are possible, affecting the observed carbon balance. Finally, the formation of SiF_4 due to the etching of the reactor wall shortens the lifetime of the reactor (Takaki *et al*., 2004), and thus careful choosing of materials to construct the reactor is necessary.

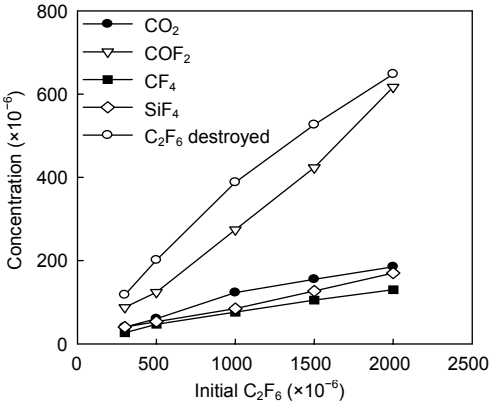

Fig. 8 Concentrations of the byproducts obtained by changing the initial C_2F_6 concentrations (oxygen: 0.5% (v/v); argon: 20% (v/v); input power: 250 W)

4 Conclusions

The C_2F_6 destruction was investigated in the dielectric-packed bed plasma reactor. The effects of the gas composition and the input power were examined and the destruction mechanisms were discussed. The electron impact dissociation is the key process for initiating the C_2F_6 destruction, which depends on the electron energy and concentration. Thus, as the input power was increased by increasing the applied voltage, the destruction efficiency was greatly enhanced. The increase in the oxygen content decreased the C_2F_6 destruction because a portion of the electrical energy delivered to the plasma reactor was consumed to form oxygen-containing byproducts. The addition of argon enhanced the C_2F_6 destruction, probably because the electron energy density distribution was shifted to favorable conditions. Regarding the effect of the initial C_2F_6 concentration, the decrease in the destruction efficiency with increasing initial C_2F_6 concentration was more significant in the absence of oxygen than in the presence of it. The C_2F_6 destruction products identified were CO_2, CO, COF_2, CF_4, and SiF_4, increasing with higher initial C_2F_6 concentrations. Judging from the distribution of these destructions products, COF_2 is the key intermediate compound leading to the formation of CO_2. A carbon balance of about 70% was achieved, indicating that other byproducts were produced from C_2F_6. The energy requirement for the C_2F_6 destruction ranged from 8.2 to 45.3 MJ/g, depending on the initial concentration.

References

Barker, J.R., 1995. Progress and Problems in Atmospheric Chemistry. World Scientific, London, UK.

Chang, M.B., Yu, S.J., 2001. An atmospheric-pressure plasma process for C_2F_6 removal. *Environmental Science and Technology*, **35**(8):1587-1592. [doi:10.1021/es001556p]

Chen, H.L., Lee, H.M., Cheng, L.C., Chang, M.B., Yu, S.J., Li, S.N., 2008. Influence of nonthermal plasma reactor type on CF_4 and SF_6 abatements. *IEEE Transactions on Plasma Science*, **36**(2):509-515. [doi:10.1109/TPS.2008.918675]

Delattre, J.L., Friedman, T.L., Stacy, A.M., 1999. Destructive abatement of CF_4 and C_2F_6 via a plasma induced reaction with CaO. *Journal of Vacuum Science and Technology B: Microelectronics and Nanometer Structures*, **17**(6):2664-2666. [doi:10.1116/1.591044]

Futamura, S., Sugasawa, M., 2008. Mechanisms for formation of organic and inorganic by-products and their control in nonthermal plasma chemical processing of VOCs. *International Journal of Environment and Waste Management*, **2**(4/5):471-483. [doi:10.1504/IJEWM.2008.021787]

Hartz, C.L., Bevan, J.W., Jackson, M.W., Wofford, B.A., 1998. Innovative surface wave plasma reactor technique for PFC abatement. *Environmental Science and Technology*, **32**(5):682-687. [doi:10.1021/es9706514]

Kucukarpaci, H.N., Lucas, J., 1979. Simulation of electron swarm parameters in carbon dioxide and nitrogen for high E/N. *Journal of Physics D: Applied Physics*, **12**(12):2123-2138. [doi:10.1088/0022-3727/12/12/014]

Lee, M.C., Choi, W., 2004. Development of thermochemical destruction method of perfluorocarbons (PFCs). *Journal of Industrial & Engineering Chemistry*, **10**(1):107-114.

Mallard, W.G., Westley, F., Herron, J.T., Hampson, R.F., Frizzell, D.H., 1998. Chemical Kinetics Database, Version 2Q98. National Institute of Standards and Technology (NIST), USA.

Mizeraczyk, J., Jasinski, M., Zakrzewski, Z., 2005. Hazardous gas treatment using atmospheric pressure microwave discharges. *Plasma Physics and Controlled Fusion*, **47**(12B):589-602. [doi:10.1088/0741-3335/47/12B/S43]

Mok, Y.S., Kim, J.H., Nam, I.S., Ham, S.W., 2000. Removal of NO and formation of byproducts in a positive-pulsed corona discharge reactor. *Industrial and Engineering Chemistry Research*, **39**(10):3938-3944. [doi:10.1021/ie000239o]

Mok, Y.S., Demidyuk, V., Whitehead, J.C., 2008. Decomposition of hydrofluorocarbons in a dielectric-packed plasma reactor. *Journal of Physical Chemistry A*, **112**(29):6586-6591. [doi:10.1021/jp8020084]

Motlagh, S., Moore, J.H., 1998. Cross sections for radicals from electron impact on methane and fluoroalkanes. *Journal of Chemical Physics*, **109**(2):432-438. [doi:10.1063/1.476580]

NIST (National Institute of Standards and Technology), 2009 Chemistry Web Book. Available from http://webbook.nist.gov/chemistry [Accessed on Oct. 15, 2009].

Okubo, M., Kametaka, H., Yoshida, K., Yamamoto, T., 2007. Odor removal characteristics of barrier-type packed-bed nonthermal plasma reactor. *Japanese Journal of Applied Physics*, **46**(8a):5288-5293. [doi:10.1143/JJAP.46.5288]

Ricketts, C.L., Wallis, A.E., Whitehead, J.C., Zhang, K., 2004. A mechanism for the destruction of CFC-12 in a nonthermal, atmospheric pressure plasma. *Journal of Physical Chemistry A*, **108**(40):8341-8345. [doi:10.1021/jp047546i]

Sun, J.W., Park, D.W., 2003. CF_4 decomposition by thermal plasma processing. *Korean Journal of Chemical Engineering*, **20**(3):476-481. [doi:10.1007/BF02705551]

Takaki, K., Urashima, K., Chang, J.S., 2004. Ferro-electric pellet shape effect of C_2F_6 removal by a packed-bed-type nonthermal plasma reactor. *IEEE Transactions on Plasma Science*, **32**(6):2175-2183. [doi:10.1109/TPS.2004.837614]

Takaki, K., Urashima, K., Chang, J.S., 2006. Scale-up of ferro-electric packed bed reactor for C_2F_6 decomposition. *Thin Solid Films*, **506-507**:414-417. [doi:10.1016/j.tsf.2005.08.104]

Tsai, W.T., Chen, H.P., Hsien, W.Y., 2002. A review of uses, environmental hazards and recovery/recycle technologies of perfluorocarbons (PFCs) emissions from the semiconductor manufacturing processes. *Journal of Loss Prevention in the Process Industries*, **15**(2):65-75. [doi:10.1016/S0950-4230(01)00067-5]

Urashima, K., Kostov, K.G., Chang, J.S., Okayasu, Y., Iwaizumi, T., Yoshimura, K., Kato, T., 2001. Removal of C_2F_6 from a semiconductor process flue gas by a ferroelectric packed-bed barrier discharge reactor with an adsorber. *IEEE Transactions on Industry Applications*, **37**(5):1456-1463. [doi:10.1109/28.952521]

Yoshida, K., Rajanikanth, B.S., Okubo, M., 2009. NO_x reduction and desorption studies under electrical discharge plasma using a simulated gas mixture: a case study on the effect of corona electrode. *Plasma Science and Technology*, **11**(3):327-333. [doi:10.1088/1009-0630/11/3/15]